Understanding Cross-Band Interference in Unsynchronized Spectrum Access

Wei Hou[†‡], Lei Yang[†], Lin Zhang[‡], Xiuming Shan[‡], Heather Zheng[†]
[†]University of California, Santa Barbara, USA, [‡]Tsinghua University, China
{weihou,leiyang,htzheng}@cs.ucsb.edu, {linzhang, shanxm}@tsinghua.edu.cn

ABSTRACT

We consider the problem of cross-band interference when devices from the same or different networks share radio spectrum. Cross-band interference occurs when unsynchronized transmissions create harmful interference among each other although they use non-overlapping frequency bands. We perform an in-depth study to analytically quantify the degree of interference and its impact on OFDMA-based packet transmissions. The analysis also takes into account practical artifacts including temporal sampling mismatch, frequency offset and power heterogeneity. Using insights from the analysis, we build and compare three methods that apply temporal and frequency redundancy to reduce the interference and add robustness against it. Experimental and analytical results show that adding frequency guardband is the most efficient solution to tackle cross-band interference.

Categories and Subject Descriptors

C.2.1 [**Network Architecture and Design**]: Wireless communication

General Terms

Algorithms, Design, Performance

Keywords

Cognitive Radios, Interference, Spectrum Access

1. INTRODUCTION

Recent advances in radio hardware design and spectrum policy have created a wide interest in dynamic spectrum access. Instead of waiting for their statically assigned spectrum, cognitive-radio devices from the same or different networks now share radio spectrum dynamically in their local neighborhood.

To dynamically access and share spectrum, the majority of devices use the orthogonal frequency division multiple access (OFDMA). It divides the available frequency bands into a large set of non-overlapping frequency subcarriers, allowing a transmission to use any combination of the subcarriers. In addition, multiple transmissions can take place simultaneously by operating on different subcarriers.

OFDMA, however, is highly sensitive to synchronization errors. Imperfect synchronization in time or frequency destroys the orthogonality among subcarriers. As a result, simultaneous transmissions will produce harmful *cross-band interference* to each other although they use different frequency subcarriers. Most prior solutions tackle this problem by strengthening the device synchronization procedure [6, 7] in cellular networks.

In this paper, we consider a "distributed" network where devices share spectrum but operate in an unsynchronized manner. To examine the impact of cross-band interference, we perform an in-depth analytical study to derive the amount of interference a subcarrier can generate and how it affects the neighboring subcarriers used by another transmission. Our analysis takes into account three key artifacts: temporal sampling mismatch, frequency offset, and power heterogeneity. For a given network topology, power and spectrum usage, the analysis produces the average interference strength experienced by any frequency subcarrier. Our results show that temporal mismatch leads to large cross-band interference that OFDMA operations cannot address.

Built on the theoretical analysis, we analyze and compare three mechanisms for tackling cross-band interference. By adding temporal and frequency redundancy to each transmission, they seek to reduce the interference at its source and to insert robustness against any interference. We analytically evaluate their effectiveness and confirm our conclusions using simulations.

Our work makes two key contributions:

(1) We build an analytical model to characterize the impact of cross-band interference on OFDMA transmissions. While prior works have examined out-of-band emission [4, 8, 11], our work is the first to analytically evaluate its impact on unsynchronized OFDMA transmissions, taking into account practical artifacts such as temporal mismatch and frequency offset. Our analytical results closely match the experimental results.

(2) Using theoretical analysis and simulation experiments,

This work was partially supported by National Science Foundation of China (Grant No. 60672107), and National Science Foundation (Grant No. 0832090).

CoRoNet'09, September 21, 2009, Beijing, China.

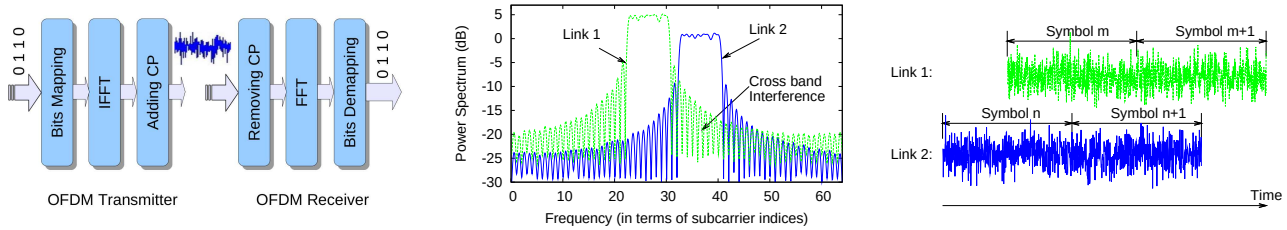

(a) OFDM block diagram

(b) Frequency domain view of two OFDMA transmissions

(c) Temporal sampling mismatch

Figure 1: Illustrating the operation of OFDMA based spectrum sharing and the impact of unsynchronized OFDMA.

we examine three mechanisms for tackling cross-band interference: frequency guardband (FGB), inter-symbol cancellation (ISC) and cross-symbol cancellation (CSC). Our results show that ISC is ineffective due to temporal mismatch, while CSC is sensitive to frequency offset. Overall, inserting frequency guardband between transmissions is the most efficient solution, because the cross-band interference degrades quickly with the frequency distance.

2. PRELIMINARY

We briefly discuss the basic operation of OFDMA and its problems when transmissions are unsynchronized.

2.1 OFDMA

OFDMA is a highly efficient mechanism to realize dynamic spectrum access and sharing. It partitions spectrum bands into many frequency subcarriers, allowing a transmission to use any combination of the subcarriers. Multiple transmissions can take place simultaneously by operating on different subcarriers.

OFDMA uses OFDM at its physical layer. As shown in Figure 1(a), each pair of devices use OFDM to transmit signals over their selected subcarriers. The transmitter maps the binary bit stream into the selected subcarriers, and applies inverse fast Fourier transform (IFFT) to convert the bit stream into time-domain OFDM symbols. In this way, it only "pours" power over the selected subcarriers. To mitigate inter-symbol interference, a cyclic prefix (CP) is appended to each OFDM symbol. The receiver extracts the time-domain symbols and applies fast Fourier transform (FFT) to reconstruct the bit stream from the intended subcarriers.

One important requirement in OFDMA is to maintain the orthogonality among subcarriers so that simultaneous transmissions from different subcarriers will not interfere with each other. Figure 1(b) shows a frequency-domain snapshot of two transmissions in an OFDMA system, in terms of the power spectrum observed by link 2's receiver. In this example, link 1 occupies subcarriers 23-30 and link 2 occupies subcarriers 33–40. We observe that both transmissions leak power to unoccupied subcarriers because of the out-of-band emission. When these transmissions are perfectly synchronized (*i.e.* their symbols start and end at the same time and their central carriers are identical), the FFT operations at their receivers will remove these unwanted signals and maintain the subcarrier orthogonality.

2.2 Unsynchronized OFDMA

OFDMA is highly sensitive to time and frequency synchronization errors because they destroy subcarrier orthogonality and create harmful interference among transmissions. Imperfect synchronization creates two artifacts: *temporal mismatch* and *frequency offsets*.

- *Temporal mismatch* (τ) refers to the difference between two transmissions' arrival time at the receiver. From Figure 1(c), we see that link 1 and 2's OFDM symbols are mis-aligned with each other when they arrive at link 2's receiver.
- *Frequency offset* (F_{off}) is the central frequency discrepancy between two transmitters, due to unaligned oscillators and varying environment. As the frequency offset within a link can be compensated at the receiver, the inter-link frequency offset dominates in unsynchronized transmissions. We assume $|F_{off}|$ is no more than 0.5 subcarrier.

In the following section, we show that these two artifacts prevent FFT operations from cancelling unwanted signals and thus destroy the subcarrier orthogonality.

3. CROSS-BAND INTERFERENCE

In this section, we examine the cross-band interference in unsynchronized OFDMA systems. Using the example in Figure 1, we treat link 1 as the interferer and examine its interference at link 2's receiver in the presence of the temporal mismatch and frequency offset. As shown by Figure 2, we divide the analysis into two cases based on the degree of temporal mismatch: $0 \leq \tau \leq T_{CP}$ or $T_{CP} < \tau < T + T_{CP}$ where T is the symbol duration and T_{CP} is its CP duration.

3.1 Case A: Small Temporal Mismatch

From Figure 2, when $\tau \leq T_{CP}$, each desired OFDM symbol will face interference from only one symbol of its interferer. Let $s(k)$ represent the frequency-domain signal sent by link 1 on subcarrier k. At link 2's receiver, it will experience a phase rotation in the frequency domain due to the temporal mismatch τ:

$$(s(k))_\tau \triangleq s(k)e^{-i2\pi\frac{k}{T}\tau} \quad (1)$$

where N is the total number of subcarriers.

To determine the cross-band interference from link 1 to link 2, we determine the power spectrum of $(s(k))_\tau$ together

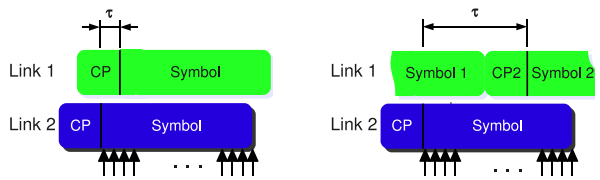

(a) Small mismatch (b) Large mismatch

Figure 2: Two temporal mismatch cases.

with the channel response at any continuous frequency $f \in [0, N)$. This allows us to determine the interference in the presence of inter-link frequency offset F_{off}, where link 1's transmissions at subcarrier #i arrive at link 2's subcarrier #i+F_{off}. For example, $f = 2$ refers to the frequency location of subcarrier #2, and $f = 2.5$ refers to the middle of subcarriers #2 and #3.

Let Ω_I represent the set of subcarriers occupied by the interferer link 1. We perform discrete-time Fourier transform (DTFT) to derive $(P^A_{1\to 2}(f))$, link 1's power spectrum seen by link 2 at any continuous f:

$$P^A_{1\to 2}(f) = |H_{1\to 2}(f) \cdot S(f)|^2 \cdot P_1(f) \quad (2)$$
$$S(f) = \sum_{k\in\Omega_I} (s(k))_\tau \frac{\sin[\pi(f-k)]}{N \sin[\frac{1}{N}\pi(f-k)]} e^{-i\pi(f-k)\frac{N-1}{N}}$$

where $H_{1\to 2}(f)$ is the frequency-domain channel response between link 1 and 2, $S(f)$ is the interferer's spectrum and $P_1(f)$ is link 1's transmission power spectrum. It is easy to show that $P^A_{1\to 2}(f) = 0$ at integer f ($f \notin \Omega_I$), plotted in Figure 3. This means that the cross-band interference can be fully cancelled if F_{off} is 0.

3.2 Case B: Large Temporal Mismatch

When $T_{CP} < \tau < T + T_{CP}$, each desired OFDM symbol will face interference from two truncated symbols (See Figure 2(b)). Without loss of generality, we assume it overlaps with symbol I in M sampling points and symbol II in $N-M$ points, where M is determined by τ. Let $s_I(k)$ and $s_{II}(k)$ represent the frequency-domain constellation points on the kth subcarrier from these symbols. Due to the temporal mismatch, each signal goes through a truncation and a phase rotation : Symbol I removes the front $N-M$ points and rotates $s_I(k)$'s phase by $-2\pi k(\tau - T)$, and Symbol II shifts its sampling location by M points to the right, removes the tail M points and rotates $s_{II}(k)$'s phase by $-2\pi k T_{CP}$.

The DTFT outputs of the two signals are:

$$\begin{cases} S_I(f) = \sum_{k\in\Omega_I} (s_I(k))_{(\tau-T)} \cdot \frac{\sin[\frac{M}{N}\pi(f-k)]}{N\sin[\frac{1}{N}\pi(f-k)]} \\ \qquad \cdot e^{-i\pi(f-k)\frac{M-1}{N}} \\ S_{II}(f) = \sum_{k\in\Omega_I} (s_{II}(k))_{T_{CP}} e^{-i2\pi f\frac{M}{N}} \cdot \frac{\sin[\frac{N-M}{N}\pi(f-k)]}{N\sin[\frac{1}{N}\pi(f-k)]} \\ \qquad \cdot e^{-i\pi(f-k)\frac{N-M-1}{N}} \end{cases}$$

And the interfering signal's power spectrum becomes:

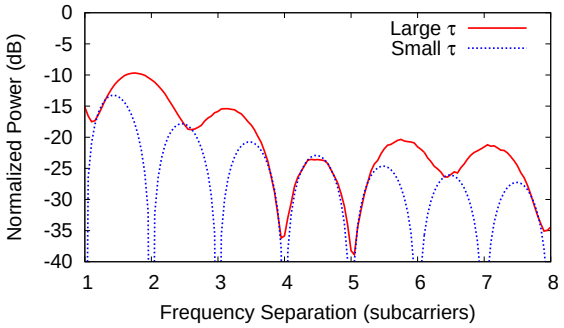

Figure 3: An example of the cross-band interference. X-axis is the frequency separation to the interferer, Y-axis is the normalized power.

$$P^B_{1\to 2}(f) = |H_{1\to 2}(f)|^2 \cdot |S_I(f) + S_{II}(f)|^2 \cdot P_1(f) \quad (3)$$

In Figure 3 we also plot the power spectrum of the interfering signal for a random τ. Because $s_I(k)$ and $s_{II}(k)$ are randomly chosen from constellation map, the power spectrum becomes randomly distributed across f and is no longer zero at integer f locations.

From the above analysis, we see that the cross-band interference depends heavily on the temporal mismatch level τ and the configuration of signals $s(\cdot)$. In unsynchronized OFDMA systems, τ becomes a random variable and so does the cross-band interference. In the following, we apply statistical analysis to derive the average interference strength.

3.3 Statistical Analysis

We derive the average interference strength at any frequency location f by averaging over the distribution of τ and $s(\cdot)$. This also allows us to examine the interference under any given F_{off}. Our analysis makes the following assumptions. Both two transmissions use the same T and T_{CP}; τ is evenly distributed in $[0, T + T_{CP})$, M is dependent on τ and evenly distributed in $[0, 1, \cdots, N-1]$; $s(k)$, $s_I(k)$ and $s_{II}(k)$ are independent and identically-distributed (i.i.d) for all $k \in \Omega_I$, randomly chosen from constellation map with unit magnitude. We assume both the channel response and transmit power spectrum are frequency flat, and denote $P_1 \triangleq |H_{1\to 2}(f)|^2 P_1(f)$. Due to the space limit, we only sketch our derivations.

For Case A, by taking an average over the i.i.d distribution of the signal constellation, the average interference strength over $s(\cdot)$ is also independent of τ:

$$E\left[P^A_{1\to 2}(f)\right] = \sum_{k\in\Omega_I} \frac{\sin^2[\pi(f-k)]}{N^2 \sin^2[\frac{1}{N}\pi(f-k)]} P_1 \quad (4)$$

For Case B, the resulting interference after averaging over $s_I(k)$, $s_{II}(k)$ and M is

$$E\left[P^B_{1\to 2}(f)\right] = \sum_{k\in\Omega_I} \frac{1 - \frac{\sin(2\pi(f-k))}{2\pi(f-k)}}{N^2 \sin^2[\frac{1}{N}\pi(f-k)]} P_1 \quad (5)$$

Based on these results, we derive the average interference strength as the probabilistic sum of those from case A and

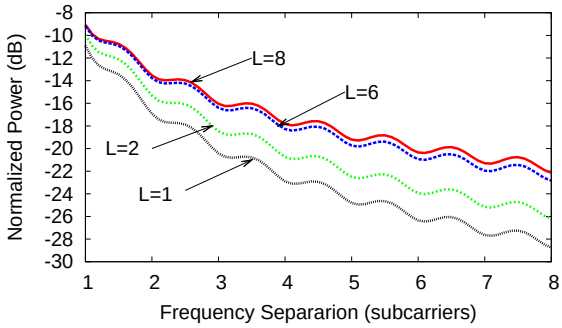

Figure 4: Average cross-band interference strength (normalized by P_1) at different frequency separation. Assuming $T_{CP} = \frac{T}{4}$.

B:

$$E\big[P_{1\to 2}(f)\big] = p_A \cdot E\big[P^A_{1\to 2}(f)\big] + p_B \cdot E\big[P^B_{1\to 2}(f)\big] \quad (6)$$

where $p_A = \frac{T_{CP}}{T+T_{CP}}, p_B = \frac{T}{T+T_{CP}}$ are probabilities of case A and B. Using the analytical result, in Figure 4 we plot the average interference strength vs. the separation between link 1 and link 2's subcarriers. The curves represent different configurations of $L = |\Omega_I|$, the total number of subcarriers occupied by link 1. These results lead to the following three key observations:

- There is no frequency location that experiences zero cross-band interference unless it is far enough from the interferer's band.
- The cross-band interference decreases quickly with the frequency-separation between links. Thus, either inserting frequency guardband between links or adding robustness in subcarriers closer to the interferer could effectively reduce its impact.
- When the interferer uses multiple subcarriers, the subcarriers closest to the desired signal produce the majority of interference. Thus controlling the signal emission at these subcarriers could effectively reduce the cross-band interference.

4. INTERFERENCE MITIGATION

Motivated by the insights from our analysis, we introduce three mechanisms to mitigate cross-band interference. By adding temporal and frequency redundancy, these mechanisms seek to reduce the interference each subcarrier leaks to its neighbors and/or to insert robustness against such interference. The first two mechanisms are from prior works and the last mechanism is our new proposal. In this section, we discuss how to analytically examine their effectiveness against the interference and our analytical conclusions, and in Section 5 we verify our conclusions using simulations.

4.1 Frequency Guardband (FGB)

Inserting frequency guardband between transmissions is the most straightforward way to mitigate cross-band interference [11]. As shown in Figure 4, the interference strength decreases with the frequency separation. For example, adding one guardband between link 1 and 2 will reduce the interference power from -8.9dB to -13.4dB. Such 4.5dB difference could significantly improve transmission quality. When a frequency guardband of l subcarriers is put between two transmissions, the cross-band interference can be derived from the original analysis by shifting $E\big[P_{1\to 2}(f)\big]$ by l subcarriers. Because guardbands are not used for transmissions, this approach leads to link overhead. The choice of l depends heavily on transmission quality and individual subcarrier usage.

4.2 Intra-Symbol Cancellation (ISC)

Another mechanism is to reduce interference strength by carefully controlling link 1's signal pattern. Prior work has proposed the *intra-symbol cancellation* (ISC) approach [9] where a transmitter codes several subcarriers within one symbol in such a way that their signal sidelobes cancel each other and hence the aggregated sidelobe becomes much smaller. For example, if a transmitter codes its subcarrier k and $k+1$ such that:

$$s(k+1) = -s(k), \quad (7)$$

then at any time-synchronized receiver, the cross-band interference from k and $k+1$ could mostly cancel each other out. With this ISC coding, the first sidelobe of the spectrum is almost 10 dB less.

This approach, however, faces two key challenges. First, it leads to extra overhead since multiple subcarriers now can only carry the load of one subcarrier. Thus choosing which set of subcarriers to code is important. Second and more importantly, ISC is highly sensitive to synchronization errors. As we have shown in Section 3, the temporal mismatch leads to different phase shifts for $s_I(k)$ and $s_{II}(k)$. Because their sidelobes cannot cancel each other, ISC will not effectively reduce the cross-band interference.

4.3 Cross-Symbol Cancellation (CSC)

To address temporal mismatch, we propose to extend coding across symbols, referred to as the *cross-symbol cancellation* (CSC). In contrast with ISC, CSC modifies two OFDM symbols on the same kth subcarrier to compensate for the temporal mismatch. Consider $s_I(k)$ and $s_{II}(k)$ defined before, after CSC, they become:

$$s_{II}(k) = (s_I(k))_{-T_{CP}} \quad (8)$$

The factor $(\cdot)_{-T_{CP}}$ compensates the phase shift so that for both Case A and B, the actual interference signal will have continuous phases, so it can be seen as one completed OFDM symbol. In this case, the aggregated signal sidelobe can be minimized at integer frequency locations. Like ISC, CSC must tradeoff the interference mitigation with the bandwidth overhead. For example, coding a small set of subcarriers on the frequency edge is more bandwidth-efficient than coding all the subcarriers together, but is less effective in tacking the interference. We skip diving into the detailed description of the CSC-based system for space limit.

Using the analytical results in the previous section, we verify that CSC is insensitive to the temporal mismatch. More importantly, the cross-band interference strength $P_{1\to 2}(f) = 0$ when $f(f \notin \Omega_I)$ is an integer of the subcarriers with full-bits coding. That is, if the frequency offset is zero, the desired signal is sampled at integer fs and does not experience any cross-band interference. On the other hand, the performance of CSC is sensitive to the frequency offset. When the

Table 1: Default Simulation Parameters

Parameter	Value
N	64
N_{CP}	16
Modulation	QPSK
Subcarrier bandwidth	12.5 kHz
Desired signal's bandwidth	8 subcarriers
Interferer's bandwidth	8 subcarriers
Packet size	32 OFDM symbols
Default guardband size	0 subcarrier

offset is 0.5 subcarrier, CSC suffers from the same interference as the original one. This conclusion is also verified in our simulation results (see Figure 5(a)).

5. EVALUATION

Using Matlab simulations, we verify the accuracy of the analytical models and evaluate the three mitigation mechanisms. By default, we simulate two links (1 and 2), each occupying 8 frequency subcarriers out of a total of 64 subcarriers. We choose $T_{CP} = T/4$ which is the standard configuration in 802.11 systems. The links are unsynchronized and start their transmissions randomly. We assume a frequency-flat and static propagation environment. Treating link 1 as the interferer, we measure its interference power at link 2's operating subcarriers, and link 2's throughput. Table 1 summarizes the default simulation parameters.

5.1 Interference Strength Measurement

Using simulations, we first generate the interferer signal and perform DTFT over the received signal at link 2. We measure the average interference power over 10,000 runs. We verify the accuracy of the analytical model by comparing it with the simulation results and measure the errors, shown in Table 2. We see that the difference between analytical and simulation results is around 0.1dB. In Table 3, we also compare them when link 1 uses different number of subcarriers, *i.e.* varying $|\Omega_I|$. The same conclusion holds.

Figure 5(a) shows the simulation results of no-mitigation, ISC and CSC, where ISC and CSC code all 8 subcarriers and have a 50% overhead. The results show that ISC leads to very little improvement and CSC can almost nullify the interference if the frequency offset is small.

5.2 Link Throughput Measurement

We use link throughput measurements to examine the impact of cross-band interference and the overhead from mitigating it. We turn both link 1 and 2 on, randomly generate 10,000 OFDM packets, each carrying 32 symbols, and measure link 2's effective throughput. We assume that the transmitter and receiver for each link are synchronized using preambles [10], but link 1 and 2 have a maximum frequency offset $F_{off} = 0.5$. We also add -40dB additive white Gaussian noise.

We compare four mechanisms: no mitigation, FGB, ISC and CSC. Because the link throughput depends on the coding overhead in ISC/CSC and the amount of frequency guardband, we configure the experiments to perform a fair comparison. Assuming a total of 16 subcarriers, we choose the best coding format for ISC/CSC to maximize its effective throughput, using the same format for link 1 and 2. For

Table 2: Average interference strength (link 1 uses subcarriers 1–8 and link 2 uses subcarriers 9–16).

Freq. sep.	$E[P_{1\to2}(f)]$ (dB) Simul.	Analysis	Freq. sep.	$E[P_{1\to2}(f)]$ (dB) Simul.	Analysis
1	−8.98	−9.05	5	−19.15	−19.21
2	−13.48	−13.54	6	−20.27	−20.34
3	−15.97	−16.05	7	−21.24	−21.30
4	−17.78	−17.83	8	−22.09	−22.13

Table 3: Comparing analytical and simulation results.

$L = \|\Omega_I\|$	4	8	16	32
Max. Difference (dB)	0.08	0.09	0.11	0.11

FGB, we place K null subcarriers between link 1 and 2, and split the rest $16 - K$ subcarriers between them. We choose the optimal K that maximizes the effective throughput.

Impact of Power Heterogeneity We examine the performance when link 2's signal is xdB stronger than link 1's signal (at their intended subcarriers). Figure 5(b) shows the results where x ranges from −9dB to 0dB when F_{off} is randomly distributed in $(-0.1, 0.1)$ subcarrier. Both CSC and FGB consistently outperform the other two. When the desired signal is −9dB weaker than the interfering signal, FGB provides up to 100% throughput improvement. FGB outperforms CSC because CSC cannot nullify the interference when $F_{off} \neq 0$ or partial bits other than all of the bits are encoded.

Impact of Frequency Offset Given CSC and FGB configurations, we examine their performance when frequency offset is uniformly distributed in $(-F_{off}, F_{off})$. Results from Figure 5(c) show that the link throughput of CSC degrades gracefully with F_{off}, especially when the desired signal is weaker. This can be explained by Figure 5(a) where the CSC's cross-band interference increases with f. When $F_{off} = 0.5$ subcarrier, the interference becomes similar to the no-mitigation case. On the other hand FGB is almost insensitive to F_{off}.

6. RELATED WORK

The problem of out-of-band emission in OFDM networks has been studied in the context of spectrum sharing among primary and secondary users [8, 11]. While existing works focus on analyzing the energy leakage observed at a primary receiver, our work provides a systematic framework to evaluate its impact on unsynchronized OFDMA transmissions.

Prior work has proposed both time-domain [4, 11] and frequency-domain approaches [1–3, 5, 9, 11] to reduce out-of-band emission. These include inserting guardand and applying windowing to reduce sidelobe power [11], and the ISC approach [1, 5, 9]. Different from these works, we focus on evaluating how out-of-band emission affects unsynchronized OFDMA transmissions, and compare different approaches using theoretical analysis and simulations. We show that ISC provides little benefit in unsynchronized systems, and propose a new CSC approach to compensate temporal mismatch.

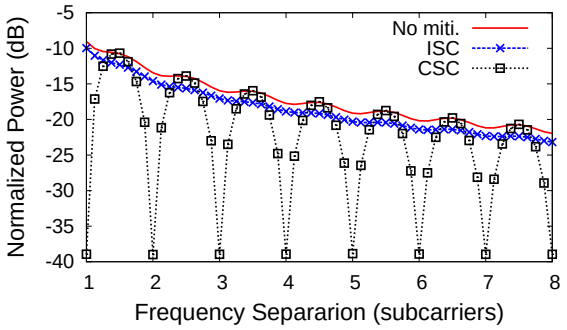

(a) Interference Measurement

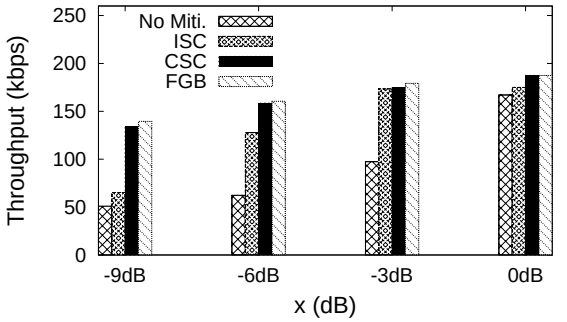

(b) Throughput Measurement

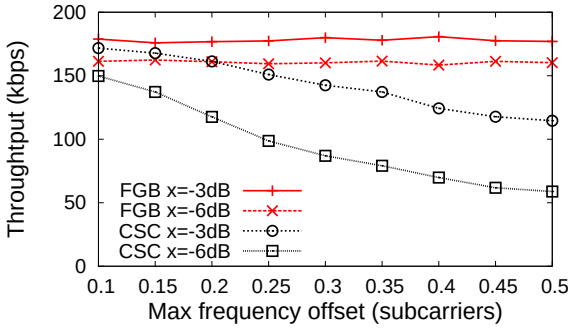

(c) Sensitivity to Frequency Offset

Figure 5: Experimental results on cross-band interference. (a) The average strength of cross-band interference at each frequency location, (b) Link 1's throughput using different interference mitigation mechanisms on both link 1 and link 2. F_{off} is uniformly distributed in $(-0.1, 0.1)$ subcarrier, (c) The link throughput under different frequency offset F_{off} using CSC and FGB.

7. CONCLUSION

We consider the problem of distributed spectrum sharing using OFDMA. Artifacts from unsynchronized transmissions destroy subcarrier orthogonality, creating cross-band interference among transmissions on non-overlapping subcarriers. We develop an analytical framework to quantify the cross-band interference and its impact on packet transmissions. To our best knowledge, our work is the first to provide an analytical evaluation of such interference in unsynchronized OFDMA systems. We then build and compare three methods to mitigate the interference. Experimental and analytical results show that adding frequency guardband is the most efficient solution in the presence of temporal mismatch and frequency offset, while the other two methods on cancelling interference are sensitive to these artifacts. We also note that the performance of frequency guardband, however, depends heavily on the guardband size. We are currently researching on selecting the optimal guardband size under various network configurations.

8. REFERENCES

[1] S. Brandes, I. Cosovic, and M. Schnell. Reduction of out-of-band radiation in OFDM systems by insertion of cancellation carriers. In *IEEE Communication Letters*, 2006.

[2] I. Cosovic, S. Brandes, and M. Schnell. Subcarrier weighting: A method for sidelobe suppression in OFDM systems. In *IEEE Communication Letters*, 2006.

[3] I. Cosovic and T. Mazzoni. Suppression of sidelobes in OFDM systems by multiple-choice sequencesy. In *European Trans on Telecom.*, 2006.

[4] H. A. Mahmoud and H. Arslanu. Sidelobe suppression in OFDM-based spectrum sharing systems using adaptive symbol transition. In *IEEE Communication Letters*, 2008.

[5] T. Matsuura, Y. Iida, C. Han, and T. Hashimoto. Improved algorithms for cancellation carrier optimization to suppress the OFDM OOB spectrum. In *IEEE Communication Letters*, 2009.

[6] M. Morelli. Timing and frequency synchronization for the uplink of an OFDMA system. In *IEEE Transactions on Communications*, 2004.

[7] H. Nguyen, E. de Carvalho, and R. Prasad. Joint estimation of the timing and frequency offset for uplink OFDMA. In *Wireless Personal Comm.*, 2008.

[8] S. Pagadarai, R. Rajbanshi, A. M. Wyglinski, and M. Gary J. Sidelobe suppression for OFDM-based cognitive radios using constellation expansion. In *Proc. of WCNC*, 2008.

[9] K. Panta and J. Armstrong. Spectral analysis of OFDM signals and its improvement by polynomial cancellation coding. In *IEEE Trans. on Consumer Electronics*, 2003.

[10] T. Schmidl and D. Cox. Robust frequency and timing synchronization for OFDM. In *IEEE Transactions on Communications*, 1997.

[11] T. Weiss, J. Hillenbrand, A. Krohn, and F. K. Jondral. Mutual interference in OFDM-based spectrum pooling systems. In *Proc. of VTC*, 2004.